Motion Control for Aerial and Ground Vehicle Autonomous Platooning

Emanuele Venzano, Hugo Pousseur, Alessandro Corrêa Victorino, Pedro Castillo Garcia

Motion Control for Aerial and Ground Vehicle Autonomous Platooning

Emanuele Venzano*, Hugo Pousseur*, Alessandro Correa Victorino*, Pedro Castillo Garcia*
*Université de technologie de Compiègne, CNRS, Heudiasyc (Heuristics and Diagnosis of Complex Systems)
CS60319 - 60203 Compiègne Cedex

***Abstract*—In this paper a navigation control for a platoon composed by a ground and an aerial vehicle is proposed. While the first one (a mobile robot, equipped with a LiDAR) visit desired points avoiding obstacles, the second one (a cheap quadrotor equipped with a vertical camera pointing to the floor) follows it both in position and orientation. The problem is related to the perception layer, autonomous visual control of the drone and autonomous control of the ground robotic vehicle. To control the quadrotor, we propose in this paper an aerial visual-servoing methodology based on an Image Based Visual Servoing (IBVS) algorithm applied to the image given by onboarded camera. A new variant of the Dynamic Window Approach methodology was developed in order to control the motions of the ground robotic vehicle. Preliminary experimental results presented show the efficacy of our aerial-ground platooning methodology.**

***Index Terms*—Quadcopter, UGV, Visual servoing, Obstacle avoidance**

I. Introduction

In the last years the research on autonomous robotic fleets has gained more and more attention. In fact, the ability of multiple agents to move and complete tasks without human intervention allows to achieve more robust, precise and difficult functions. Between all the possible fleets, heterogeneous systems are very popular since they can exploit the advantages of different robots.

In particular, driving of aerial vehicles has seen great developments thanks to their relative low costs, efficiency and agility. The ability to hovering, as well as vertical take off and landing have made the quadrotors one of the most used vehicles in the fields of inspections, surveillance, search-and-rescue and disaster response. On the other hand, ground vehicles are very popular because of their ability to carry heavy loads, cope with different weather conditions and drive for longer periods and distances.

The aim of this work is to define a platooning system that exploits the advantages of both types of robot: while the aerial drone is faster and is not constrained to the floor, the ground robot can be equipped with heavier and more powerful sensors. The objective is to define sensor based control for both aerial and ground agents. In particular, the leader of the platoon is the ground vehicle, which navigates in the environment using LiDAR and odometry sensor, while the follower is a quadrotor UAV, that is controlled with an IBVS (image-based visual servoing) methodology based on the visual perception of ground robot and its environment provided by a vertical onboarded camera. Cooperation between aerial and ground vehicle was used to map a 3D environment [1] and identify threats [2]. Moreover, it was used for navigation purposes in different scenarios, both in indoor [3] and outdoor [4] environments.

In literature many studies relies on GPS sensor, which allows to estimate the position of the agent in a global frame. However, this sensor is not always available (for example in indoor environments), could be inaccurate (as it happens in dense urban area where buildings could hide some satellites) and does not fit well tracking applications (not providing the relative distance to the target, the target's GPS position should be continuously sent to the follower). Because of their reliability, cheap cost and the possibility to be used in both indoor and outdoor environments, camera sensors are more and more used in this research field and images are used in the control of autonomous vehicle.

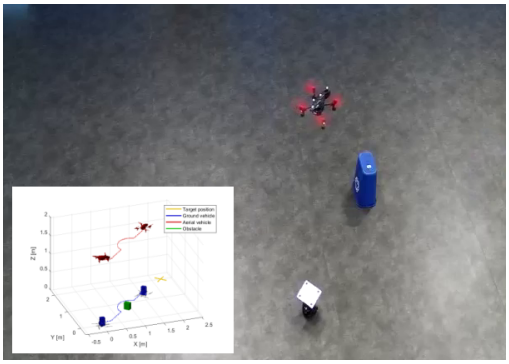

Fig. 1: Overall scheme of the scenario addressed in this work. The ground vehicle moves from the initial position to the target one avoiding the obstacle. The aerial vehicle follows the ground one maintaining it in the field of view

Visual servoing approach was chosen to define control references exploiting features in the drone camera image. Within this class of algorithms, two different methods could be identified: Position Based Visual Servoing and Image Based Visual Servoing. The first one requires to compute the relative pose between the camera and the object and it was used in [5] where a ground vehicle was equipped with a camera to provide to a UAV its relative pose. The relative pose was also used in [6] and [7], but in those cases the camera was onboard the drone. Since PBVS is sensitive to camera calibration errors and

shows a tendency for image features to leave the camera field of view, the IBVS was preferred in this work. This algorithm was used in [8] where it was applied on a UAV to achieve a desired position with respect to a ground vehicle equipped with a QR code target.

The ground vehicle must exploit the above cited sensors to navigate its environment. The use of a local planner in the UGV is necessary for the robot to safely plan the path to the goal. We chose to use an approach inspired by the Dynamic Window Approach (DWA) [9] because of the smoothness of the motion and ease of implementation [10] [11].

In this work an original approach to the cooperative navigation of ground and aerial vehicle is proposed. Indeed the agents compose an autonomous platoon where the ground vehicle is the leader and the drone follows and observe it from above. While for the first agent a variation of the DWA method is used, the quadcopter exploits velocity references from IBVS with a non pan-tilting vertical camera.

The paper is organized as follows: in section II the problem addressed in this work is presented. In section III and IV the control strategies used on the aerial and the ground vehicle are explained. In section V the experimental scenarios and the obtained results are shown. Finally, conclusions about the work are drawn and further developments are proposed in section VI .

II. Problem Statement

The purpose of this work is to address the problem of autonomous platooning of a ground and an aerial vehicle. In particular, the ground vehicle was wanted to autonomously move to reach some target points while avoiding ground obstacles. Odometry sensors were used to estimate the ground vehicle position, while LiDAR sensor was used to identify and avoid obstacles.

At the same time, the aerial vehicle exploited a sensor based control to hover and track the ground vehicle during the displacement. In this case, the vertical camera of the drone, as well as ultrasounds and Altitude and Heading Reference System (AHRS) sensors were used to track the ground vehicle maintaining a constant relative altitude.

In Fig. 1 the scenario studied in this work is presented. At the beginning, the ground vehicle is assumed in the field of view of the aerial one. When a desired target position is sent to the ground vehicle, the latter starts moving to achieve it. At the same time, the aerial vehicle follows the UGV both on the position and the orientation. If some obstacles are put in the trajectory of the ground vehicle, it detects them with the LiDAR and change its path to avoid them. The motion control methodologies applied to these heterogeneous aerial-ground robotic system two are described in the next sections.

III. Aerial Vehicle Control

The aerial vehicle control is based on the inner/outer control scheme, as shown in Fig. 2. While the outer loop (colored in blue) defines some references with a low rate, the inner loop (in color red) works at high frequency to follow the references. The IBVS method [12] was used to compute velocity control inputs to the drone, in x, y and yaw dimensions. These control inputs are computed each outer loop step based on the minimization of target features in the image plane of the onboarded vertical camera.

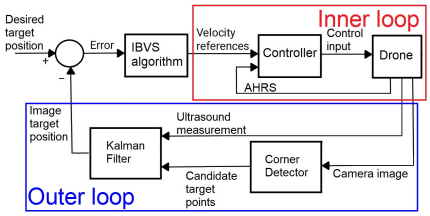

Fig. 2: Inner/outer loop scheme and sensor used for the navigation of the aerial drone

Due to image acquisition and processing, this loop operates about 60Hz. In order to simplify the detection of the ground vehicle in the camera image, a predefined target was applied on it. The proposed target was defined as a white plane with four black points placed at the corners of a fictive square.

Within the outer loop, a Shi-Tomasi corner detector [13] was applied to the image to identify the four points. To improve the identification, a Kalman Filter which takes into account the known shape of the target was used. The filter is initialised using the four points that better fits the shape of the target. Moreover, the ultrasounds sensor was used to estimate the expected dimension of the target from the current altitude. Once the filter was initialised, it was updated with the measurements from the following images, using the detected corners enough close to the points estimated within the filter. If it was not possible to identify the four points for a predefined number of following images, the filter was reinitialised as the first time.

IBVS algorithm was applied to the points given by the Kalman filter to define the reference velocities along x, y and yaw. It was decided to not use the reference along z since a relation between this reference and the relative orientation was observed. Indeed, from the same relative position different references along z were obtained changing the relative orientation between the agents. Computing the reference v_z along z it was found:

$$v_z = \lambda \, z^* \, p_a \left(\frac{\cos(p_\theta)}{a} - 1 \right)$$

where λ is the IBVS convergence parameter, z^* is the desired altitude, a is the desired dimension of the target, p_a and p_θ are the dimension and the orientation of the current target in the image plane.

A position control was considered exploiting ultrasounds sensor to estimate the altitude of the drone but, because of the different objects considered in the work (ground vehicle, obstacles and ground), poor performances were observed.

Because of these reasons, in this work it was chosen to control the altitude with the position given by the laboratory camera system.

On the other hand, both the x and y position and the yaw orientation were controlled with the sensor based scheme proposed in this work. Once the reference from IBVS was computed, it was passed to the inner control loop (which runs about 200Hz).

Here, the error between the yaw angular velocity given by AHRS sensor and the reference from IBVS was minimized to align the aerial and ground vehicle orientations. Since it was not possible to precisely measure the x and y velocities, a different approach was used along these two axes: it was observed that the x and y IBVS references were related with the relative position error. Analyzing the equation of the references it was shown that those references were proportional to the relative position error:

$$v_x = \lambda\, z^* \;\frac{1}{4}\sum_{i=1}^{4} {}^{i}p_x \qquad v_y = \lambda\, z^* \;\frac{1}{4}\sum_{i=1}^{4} {}^{i}p_y$$

where ${}^{i}p_x$ and ${}^{i}p_y$ are the coordinates of point i along x and y respectively.

These formulas confirmed that when the ground vehicle was ahead along x, the IBVS reference and the relative position error along this axis were positive, while they were zero if the two agents had exactly the same coordinate. In order to avoid oscillations and ensure good tracking performances, both the IBVS reference and its derivative were used in the control for both x and y.

A backstepping control was applied that minimizes the error between the current and the desired angular velocity, the position error along z and the references (hence the relative position error) for x and y. Experimental validations, shown in section V, demonstrate the efficacy of the proposed IBVS control method.

IV. Ground Vehicle Navigation

The ground vehicle must travel to certain positions defined before the experiment and the robot is in a location with obstacles.

The robot implements a variant of the Dynamic Window Approach (DWA) [9]. The DWA is an online avoidance obstacle, capable of achieving a goal by avoiding obstacles around it. This new approach implements the same concepts as the original proposal but the way of defining the optimal solution is different. This version replaces the brute force method with a convergence method to reduce the complexity and therefore the execution time.

A. Objective function to Loss function

This implementation requires changing the objective function (Eq 1) into a convex loss function. The initial approach is composed of sub-functions, each allowing to quantify a velocity.

$$\begin{aligned} G(v,w) =& \alpha.heading(v,w) \\ &+ \beta.dist(v,w) \\ &+ \gamma.velocity(v,w) \end{aligned} \tag{1}$$

The function $heading$ quantifies whether the robot will be close to the goal or not, the function $dist$ quantifies whether the robot will be far from obstacles or not and the function $velocity$ quantifies whether the robot is close to the desired speed.

The selected velocity is the velocity in the search space (IV-B) that maximizes the objective function. But this approach requires evaluating each velocity in the search space. This approach is costly in complexity.

In our approach, we replace the objective function with a loss function. This loss function is constructed using the same approach as the objective function, and each subfunction is a convex loss function. Then we can apply this following convex property:

> if $w_1, ..., w_n \geq 0$ and $f_1, ..., f_n$ are all convex, then so $w_1 f_1 + ... + w_n f_n$ is convex.

This the final function is convex and is defined as Eq 2.

$$\begin{aligned} L(v,w) =& \alpha.heading_{loss}(v,w) \\ &+ \beta.dist_{loss}(v,w) \\ &+ \gamma.velocity_{loss}(v,w) \end{aligned} \tag{2}$$

With this new definition, we can apply a gradient descent on the loss function and select the best velocity.

B. Search Space Limitation

The initial DWA approach limits the search space velocity. This space defines all attainable velocities of the robot for a time t. A velocity is defined as attainable if the acceleration or deceleration of the robot is sufficient and if the robot does not collide with an obstacle.

It is important to keep this concept in our approach. Our idea is to apply gradient descent until the velocity is in the search space. Once the gradient descent is out of this space, we select the previous value. The following Figure 3 shows how gradient descent engages and stops.

V. Experimental results

Experiments were conducted to show the behaviour of the system composed by the two agents. The ground vehicle is the leader of the platoon and displace itself to visit some specified set-points avoiding obstacles. At the same time, the aerial vehicle follows it observing the space and exploiting the proposed sensor-based control.

During experimental tests, a Turtlebot 3 equipped with Odometric sensor and LiDAR was used. In order to identify the vehicle in the aerial drone camera image, an additional layer was put over the Turtlebot. On top of it, a target

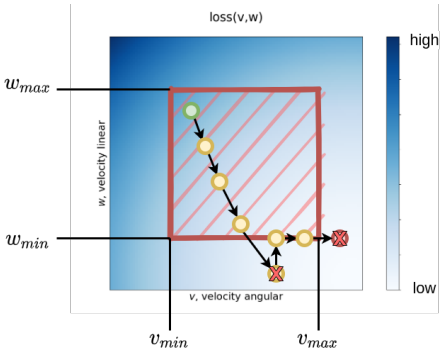

Fig. 3: Gradient descent limitation

composed by four points was placed. The robot is shown in Fig. 4.

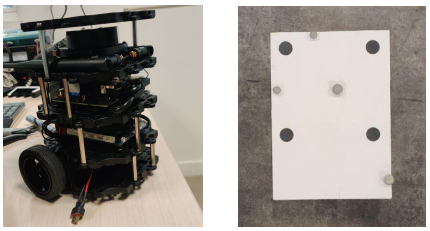

(a) Vehicle front view (b) Vehicle bird view

Fig. 4: Ground vehicle used during experimental tests. The vehicle was equipped with an extra layer on which a four points target was placed to facilitate vehicle recognition

For the aerial drone it was chosen to use the Parrot AR.Drone 2.0 shown in Fig. 5. This drone is equipped with a vertical camera running at 60 fps with 320x240 pixels resolution. Moreover, this drone was already equipped with Ultrasounds and AHRS sensors.

Fig. 5: Aerial drone used during experimental tests. Some reflective markers were put on the drone to be recognised by the OptiTrack camera system

In Fig. 6 is shown the scene perceived by the drone during flight and the target identified in the image. The blue crosses represent the corners identified through Shi-Tomasi detector, while the light blue square represents the four points chosen as belonging to the target.

To analyze and plot the behaviour of the robots during the experiments, OptiTrack camera system of the laboratory was used to obtain the position of the agents and the obstacles. For

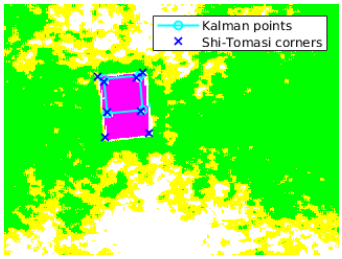

Fig. 6: Image taken from the drone in which the perception of the target is highlighted

this reason, high reflective marker balls were placed over the drone and the target.

Two different test scenarios were analysed: in the first one the main focus was about the ability of the two agents to handle different obstacle configurations, while in the second one more attention was put in respecting a predefined trajectory.

A. *Different obstacle configurations*

During the first test the target points were placed to suggest a triangular movement of the agents. During the first edge, one obstacle was placed between the initial position and the first target position to observe how the system surrounded obstacles. In the second edge two obstacles were placed to check if the agents were able to pass in the middle of them while during the third edge no obstacles were placed, to study how the system behaves in open field.

In Fig. 7 the test scenario is shown. In color red the aerial vehicle and in color blue the turtlebot are shown at their initial positions. In color green the three obstacles are shown and in color yellow the target position are drawn.

In Fig. 8 the trajectories of the aerial and ground vehicle with respect to the target points and the obstacles are shown. In particular, it is interesting to note how the ground vehicle changed its trajectory (colored in blue) to avoid the obstacles while achieving the desired points. At the same time, the trajectory of the drone is shown in color red.

In Fig. 9 the position of the agents along x and y axes are shown. Even if in Fig. 8 the position of the drone could seem quite far from the one of the turtlebot, Fig. 9 shows, in a qualitative way, that the drone well followed the ground vehicle.

In Fig. 10 the yaw orientation of the two agents is shown. From this image it is possible to see that the sensor based algorithm made the aerial vehicle achieve good performances not only for the x and y coordinates, but also for the yaw orientation. Moreover, it is possible to observe some spikes in the orientation of the turtlebot. Since this behavior was not seen in real time, those inaccuracies were probably due to imprecise identification of the target from OptiTrack. For completeness of analysis, also the altitude of the aerial vehicle and the target placed over the turtlebot are shown.

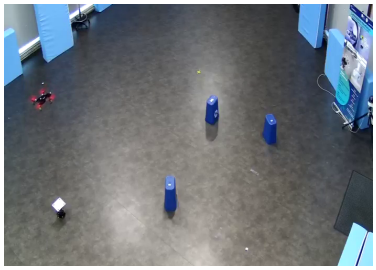

(a) Snapshot of experimental test video recording

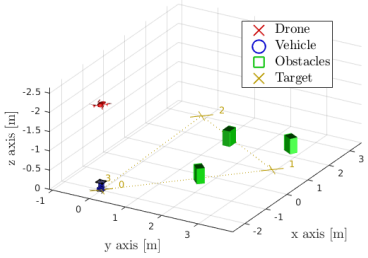

(b) 3D reconstruction of experiment scenario

Fig. 7: Experimental scenario in which it was studied how the system handle different obstacle situations

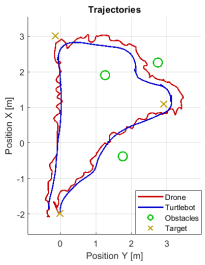

Fig. 8: Experimental trajectories of the agents dealing with different obstacle configurations

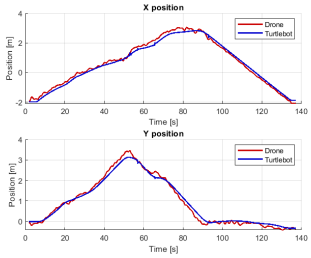

Fig. 9: Trajectory of aerial and ground vehicle along x and y axes

B. Desired trajectory

During the second experiment, more target points were used to suggest a desired trajectory for the agents. In this case, the obstacles were not placed within the trajectory on purpose, but were used in a more natural way: while the turtlebot moves accordingly to the desired target points, it should also avoid collision with some obstacles in the space. In Fig. 11 the

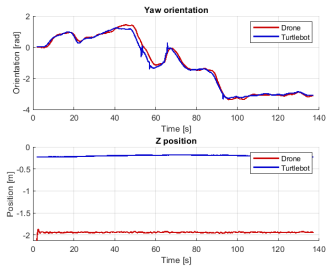

Fig. 10: Orientation and altitude of aerial vehicle and ground vehicle target along time

obstacles and target points are shown.

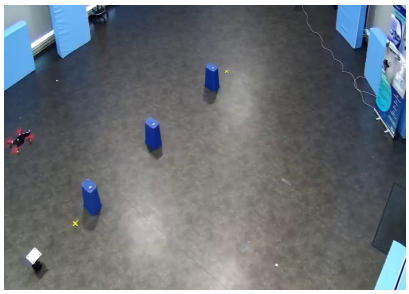

(a) Snapshot of experimental test video recording

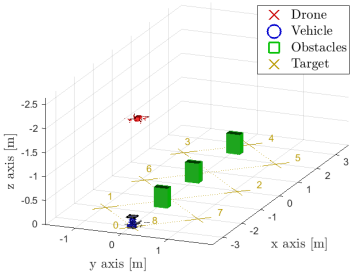

(b) 3D reconstruction of experiment scenario

Fig. 11: Experimental scenario. The initial position of aerial and ground vehicle are shown, as well as target points belonging to the desired trajectory and obstacle positions

In Fig. 12 the trajectories of the ground and aerial vehicle are shown. As it is possible to see, the ground vehicle passed close to all the target points and modified its path to avoid obstacles. This behaviour is clear to see when the ground robot moves from set-point 6 (in position [0,-1]) to set-point 7 (in position [-2,1]). At the beginning the robot moved directly to set-point 7, than it had to turn to avoid the obstacle placed between them.

In Fig. 13 the coordinates of the two agents along x and y axes are shown. Comparing the two trajectories, it is possible to notice that the aerial vehicle well followed the path of the turtlebot. Some inaccuracies are present, but the overall behaviour is reasonable with the goal of the work.

In Fig. 14 the orientation of the two agents is shown. Also in this case, the performance of the following control works

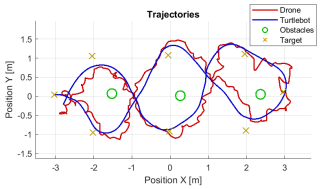

Fig. 12: Agents trajectories with respect to target points and obstacle positions

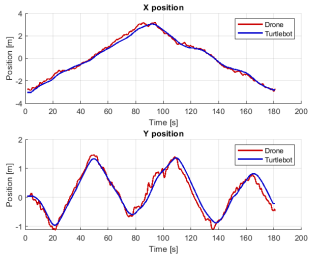

Fig. 13: Aerial and ground vehicles positions along x and y axes during the experiment

well making the drone turn as the ground vehicle. As for the previous experiment, the altitude of the agents is shown for completeness of analysis.

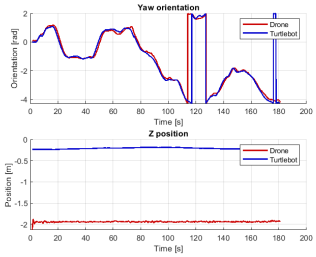

Fig. 14: Orientation and altitude of the agents during the experiment

VI. Conclusions and Perspectives

The platooning system showed good performances in all the tested scenarios. This experimentation was an opportunity to implement our new version of DWA on a real robot and to test the IBVS control applied to the UAV.

As expected, the robot avoids obstacles and passes through the given positions. During the experiment, the robot performs about 5 iterations per calculation showing its performance. Furthermore, while the ground vehicle visited the specified set points, the drone followed the other agent well by exploiting the sensor-based control.

Experimental results using real robots were performed, which show that the IBVS control made the drone well follow the ground vehicle even if moving along different trajectories and with different velocities. Not only the references were correctly computed, but they were also properly exploited for the navigation purpose. However, the behaviour of the drone along z was controlled through the position obtained via OptiTrack cameras. A further study will focus on this axis to maintain the drone at a desired altitude. This way, the system will be able to work also in spaces not provided with specific equipment.

The natural improvement of the work will be to develop cooperation between the agents to exploit the employment of two different robots. In fact, it would be possible to use the bird view of the aerial vehicle to analyze the space around the ground vehicle. Processing the image of the drone's camera could result in position set-points for the ground vehicle if the same ground vehicle control was used. Otherwise, heading and velocity references could be computed and sent by the drone to the other robot. This way, the cooperation would be used for ground vehicle navigation aid.

References

[1] H. Qin, Z. Meng, W. Meng, X. Chen, H. Sun, F. Lin, and M. H. Ang, "Autonomous exploration and mapping system using heterogeneous uavs and ugvs in gps-denied environments," *IEEE Transactions on Vehicular Technology*, vol. 68, no. 2, pp. 1339–1350, 2019.

[2] C. Reardon and J. Fink, "Air-ground robot team surveillance of complex 3d environments," in *2016 IEEE International Symposium on Safety, Security, and Rescue Robotics (SSRR)*, pp. 320–327, 2016.

[3] Q. Wu, J. Qi, C. Wu, and M. Wang, "Design of ugv trajectory tracking controller in ugv-uav cooperation," in *2020 39th Chinese Control Conference (CCC)*, pp. 3689–3694, 2020.

[4] M. Mammarella, L. Comba, A. Biglia, F. Dabbene, and P. Gay, "Cooperative agricultural operations of aerial and ground unmanned vehicles," in *2020 IEEE International Workshop on Metrology for Agriculture and Forestry (MetroAgriFor)*, pp. 224–229, 2020.

[5] J. Li, W. Dong, S. Sheng, and S. Xu, "Visual servoing of micro aerial vehicles with the cooperation of ground vehicle," in *2020 IEEE/ION Position, Location and Navigation Symposium (PLANS)*, pp. 150–155, 2020.

[6] W. Zhao, H. Liu, F. L. Lewis, K. P. Valavanis, and X. Wang, "Robust visual servoing control for ground target tracking of quadrotors," *IEEE Transactions on Control Systems Technology*, vol. 28, no. 5, pp. 1980–1987, 2020.

[7] X. Xiao, J. Dufek, and R. Murphy, "Visual servoing for teleoperation using a tethered uav," in *2017 IEEE International Symposium on Safety, Security and Rescue Robotics (SSRR)*, pp. 147–152, 2017.

[8] J. Gomez-Avila, C. Lopez-Franco, A. Alanis, N. Arana-Daniel, and M. Lopez-Franco, "Ground vehicle tracking with a quadrotor using image based visual servoing," *IFAC-PapersOnLine*, vol. 51, pp. 344–349, 01 2018.

[9] D. Fox, W. Burgard, and S. Thrun, "The dynamic window approach to collision avoidance," *IEEE Robotics and Automation Magazine*, vol. 4, no. 1, pp. 23–33, 1997.

[10] I. Naotunna and T. Wongratanaphisan, "Comparison of ros local planners with differential drive heavy robotic system," in *2020 International Conference on Advanced Mechatronic Systems (ICAMechS)*, pp. 1–6, IEEE, 2020.

[11] B. Cybulski, A. Wegierska, and G. Granosik, "Accuracy comparison of navigation local planners on ros-based mobile robot," in *2019 12th International Workshop on Robot Motion and Control (RoMoCo)*, pp. 104–111, IEEE, 2019.

[12] F. Chaumette and S. Hutchinson, "Visual servo control, Part I: Basic approaches," *IEEE Robotics and Automation Magazine*, vol. 13, no. 4, pp. 82–90, 2006.

[13] J. Shi and Tomasi, "Good features to track," in *1994 Proceedings of IEEE Conference on Computer Vision and Pattern Recognition*, pp. 593–600, 1994.